The Study of PD Propagation Phenomenon in Power Network

Qin Shaozhen and S. Birlasekaran, *Senior Member, IEEE*

***Abstract*—This paper presents the measured and analyzed responses of the partial discharge (PD) when it propagates in a power network from its origin to the measuring nodes. On and offline measurements are done in a power network consisting of a 16.5-kV/250-MVA-rated power generator, busbar, and step-up transformer. The simultaneously measured PD at two ends of the busbar indicated that the intensity of PD decreased as it traveled a longer distance and the time interval of its occurrence had a finite delay indicating the dominant mode of PD propagation as a transmission line. Frequency-domain analysis indicated the presence of characteristic resonance frequencies and the number increased as the measuring node moved away from the PD origin. The offline measurement by injecting an exponential PD signal at the neutral indicated that the signal will be absorbed in the generator, and the signal at the measuring node will be attenuated by 50 times and will be distorted. Pspice simulation is used to develop the network model for the propagation path. The Pspice analysis indicated that the distributed models of generator, busbar, and lumped parameter models of a transformer can be used to match the offline measurement. The model showed that each model can have the characteristic resonant peaks depending on the selected parameters and it can distort the simultaneously observed PD at two different nodes.**

***Index Terms*—Busbar, generator, partial discharge (PD), propagation, simulation, transfer function, transformer.**

I. Introduction

PARTIAL-DISCHARGE (PD) testing has long been used to evaluate the quality of high-voltage electrical insulation [1]. Pulse propagation [1] is frequency dependent.

The types of PD in machine windings and the various detection methods have been discussed above. The interpretation of PD test results to identify the type of developing PD and the location of the PD source based on single-pulse PD analysis is the current field of research for the complex construction such as generators. Pulse propagation study using wideband pulse response tests on stator windings has shown that a fast rise-time pulse is capacitively coupled through the winding, and that this is followed by a slower electromagnetic (EM) traveling wave. In many windings, the fast rise-time, capacitively coupled pulse is subject to rapid attenuation. Generally, the conventional models developed to treat pulse propagation are not applicable at the frequencies (>100 MHz) implied by this type of coupling. At such high frequencies, stray and interconductor capacitances become increasingly important. These capacitive effects are generally ignored by the low-frequency treatments [1]. Concerning the slower, EM traveling wave, the stator winding is treated as a transmission line, with each coil or bar having an associated inductance or capacitance. Depending on the length of each coil or bar and the number in each parallel circuit, every winding will possess a unique set of resonant frequencies. If the pass band of the sensor/detector system coincides with one of these frequencies, the magnitude of the measured PD will be abnormally high [1]. Pulse propagation in windings and the associated calibration issues is extensively researched to understand the distortion introduced by the complex windings. The characteristics of the winding [2] are visualized as a transmission line with a surge impedance of around 30 Ω and with a capacitance to ground on the order of 5 nF within the slot. Outside the slot, the end winding's surge impedance is not defined well. The effect of resonant frequencies and transmission-line phenomenon in attenuating and distorting a PD signal through the complex inductive-capacitive winding network is explored [2]–[4]. Fast-rise-injected PD pulses are found to give many resonant frequencies [3]. Reference [5] discusses the development of a simulation model to study the propagation of PD pulses in the transformer network of a 500-kV substation. The transformer is modeled as a distributed network and the parameters are computed using geometrical data. For Electromagnetic Transients Program (EMTP) analysis, this model of the transformer network is used with the capacitive model of various connected current transformers (CTs) and capacitive voltage transformers (CVTs). The entire substation network was included to calculate the PD propagation through the transformer. References [6]–[9] use a transmission-line model with frequency-dependent parameters to study the propagation of PD pulses in transformer windings. The location of injected PD using simulation is identified by zeros of the derived transfer function. By using phase comparison studies with the transfer function analysis on two nodes, the propagation path is found to influence PD measurements [10]. After a series of measurements in a generator stator winding, PD is found to propagate as a traveling wave [11] and high frequencies in the order of hundreds of megahertz are highly attenuated. Su [12] recommends modeling the stator winding as a ladder network of inductances covering the slot-turn, end-turn, and mutual inductances between the end-turns and capacitances covering the slot-turn, end-turn, and coil-to-coil capacitances in the end-turns. Su predicted from his measurements that the PD pulse can propagate through a stator winding at different speeds depending on the frequency content. The maximum limit for the traveling-wave mode of propagation was 160 kHz.

Manuscript received May 4, 2005; revised July 16, 2005. Paper no. TPWRD-00256-2005.

Qin Shaozhen is with the Condition Monitoring Group of Singapore Power Power Grid, Singapore 238164 (e-mail: shaozhen@singaporepower.com.sg).

S. Birlasekaran is with the School of Electrical and Electronic Engineering, Nanyang Technological University, Singapore 639798 (e-mail: ebirla@ntu.edu.sg).

Digital Object Identifier 10.1109/TPWRD.2005.860282

From the injection of simulated PD on a 35-MW stator, two modes of PD propagation [13] are observed. The slow mode with a propagation velocity of 9 m/μs is attributed to the traveling-wave component, and the fast mode through the end windings is observed due to the EM coupling at the terminals without much delay.

The high-frequency components are highly attenuated with the PD propagation length of the winding [10]. The traveling-wave speed increases with frequency in the low-frequency band up to 60 kHz and in the high-frequency band above 120 kHz. The speed is constant from 60 to 120 kHz [12]. The measured response in a transformer due to an exponential injected PD signal can be categorized into three components [14]: capacitive component (0.1–10 MHz), traveling-wave component caused by EM wave transmission (0–0.01 MHz), and an oscillating component caused by the LC circuit of the insulating system that was excited by PD (0.01–0.1 MHz). The windings acted as a low-pass filter, the cutoff frequency being dependent on the winding length and being below 1 MHz.

In rotating machine stator windings [2], the initial pulses are significantly distorted and attenuated as they propagate through a winding. The attenuation at frequencies above 35 MHz is much stronger. The lower frequency components seem to be less attenuated than the high-frequency components. The cause of this frequency-dependent response is attributed to the L–C nature of a stator winding.

Reference [15] simplified the transmission-line model of a generator winding to a second-order R, L, and C network for overvoltage analysis. Reference [16] develops a model using EMTP to predict the interturn voltage on the generator winding.

However, while much work was done on the simulated model and separate equipment, very little work was done on the propagation characteristics of PD in a real power generator operating in the power station.

The reported propagation modes for PD are the transmission-line mode [6]–[8], fast-mode EM coupling at the end windings [13], capacitive coupling between turns [14], oscillatory mode due to the LC path of the winding [14], and multiconductor transmission modes [9], [12].

The transformer model [5]–[9], [14] often considers mutual inductance between different parts of the winding, but the generator model [12], [15], [16] is due to the arrangement of the coils in individual slots, so that the influence of the mutual capacitance and the mutual inductance between different parts of the winding is small [17], [19]. The biggest differences between such machines and transformers of comparable rating are that there are fewer turns but longer and are deeply buried in the stator steel. The capacitance to ground is comparatively high, but series capacitance effects are only significant where conductors occupy the same slot [18]. As the geometrical configuration is different, the model parameters are different.

The surge impedance of the winding is about 5–45 kΩ for the winding. The measured surge impedances of rotating electrical machines are from 60 to 1600 Ω. It is apparent that the surge impedances are much smaller with rotating machines than with transformers [17]. The winding behaves more like a transmission line with relatively high surge impedance, on the order of 1000 Ω [18].

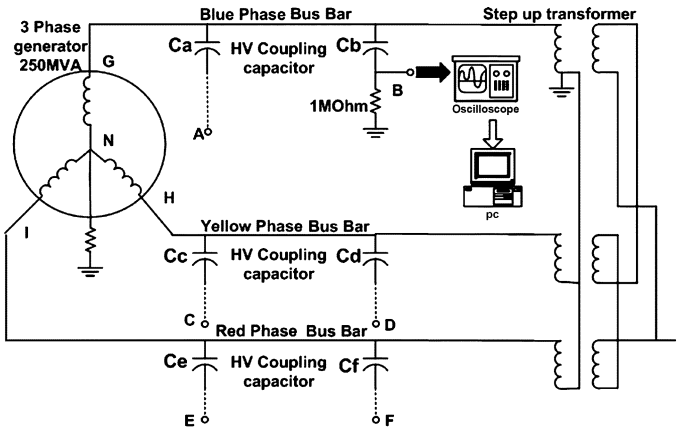

Fig. 1. Measurement setup.

In this work, the portable PD pulse sources were developed using a mercury switch to generate the PD pulses. A computerized high-frequency measurement system was developed and tested for PD propagation studies on the generator at a power plant. The online and offline testing was done on the generator. The suitable model to match the test results was analyzed.

II. Layout of the Measurement Setup

For PD propagation studies, a local power-generating station network was used as shown in Fig. 1 that consisted of a 16.5-kV/250-MVA-rated generator connected to a step-up transformer of 16.5 kV/220 kV using a 25-m-long busbar. Both on and offline PD measurements were made. High-voltage coupling epoxy-mica capacitors (Ca,. . .,Cf) 80 pF/25 kV were available on all of the three-phase terminals at the two ends of the busbar. By terminating with a suitable resistor in series with the LV end of the capacitor and ground, PD signals can be monitored simultaneously using a high-speed four-channel digital oscilloscope with a maximum sampling rate up to 5 GSamples/s. In the first series of experiments, online measurements of simultaneously occurring pulses were recorded in a 20-ms period at nodes A, C, and E of all three phases. Observed electromagentic-interference (EMI) noises, denoising methods to extract PD distribution in 20 ms and the shape of single PD were reported in another paper [20]. After evaluating the dominant time-domain PD signals in the red phase, simultaneous measurements were made at the E and F terminals of the red phase to characterize the PD propagation from the generator end to the transformer end. In the second series of experiments, a portable PD pulse source was developed using a mercury switch. The rise time of the generated exponential PD was 200 ns and the fall time was 600 ns with a peak magnitude of 25 V. In offline mode, this PD was injected at I and N of the generator winding terminals and the responses at E and F terminals were recorded simultaneously.

III. Measurement Results

A. Online-Measured PD Data

Since the main objective of the research was to identify the PD propagation phenomenon in a power network, the characteristics of simultaneously recorded online single PD data at E

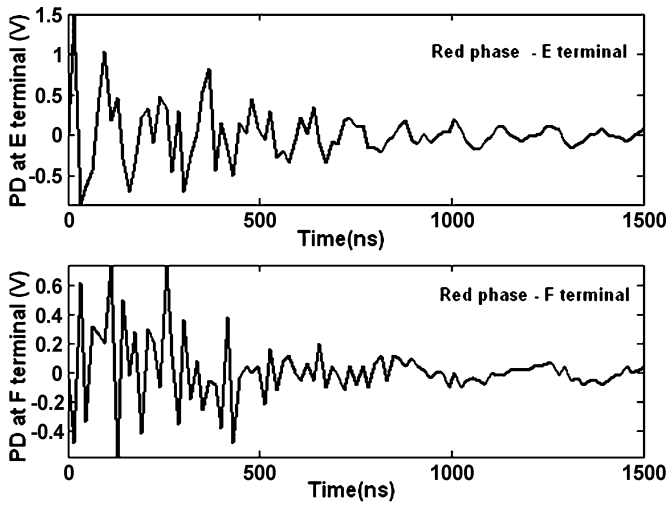

Fig. 2. Simultaneously recorded single PD pulse (17th in Fig. 3) at the E terminal (top) and F terminal (bottom) of the network.

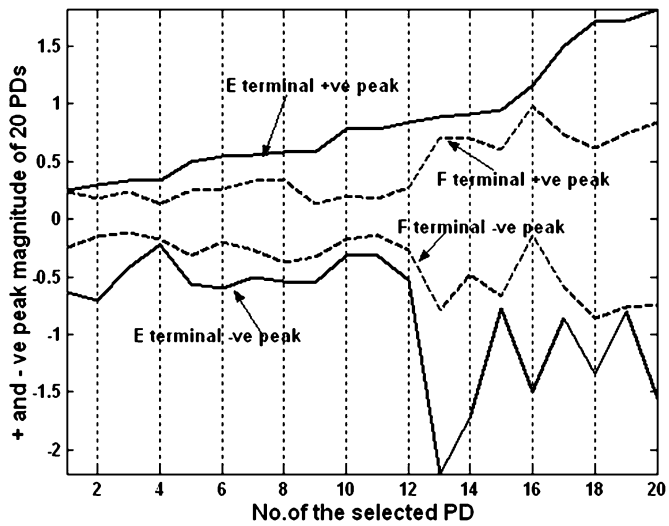

Fig. 3. Sorted by E terminal +ve peak on 20 PD pulses. (+ve and −ve peak magnitudes at the E and F terminals are shown).

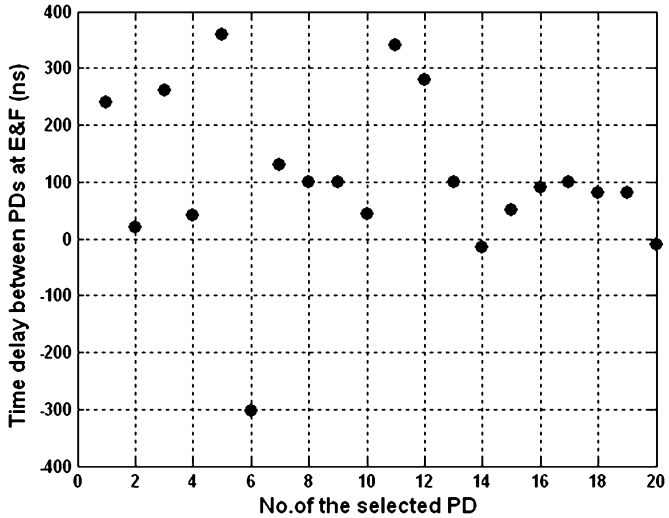

Fig. 4. Time delay of peak occurrence at the E and F terminals for 20 single PDs.

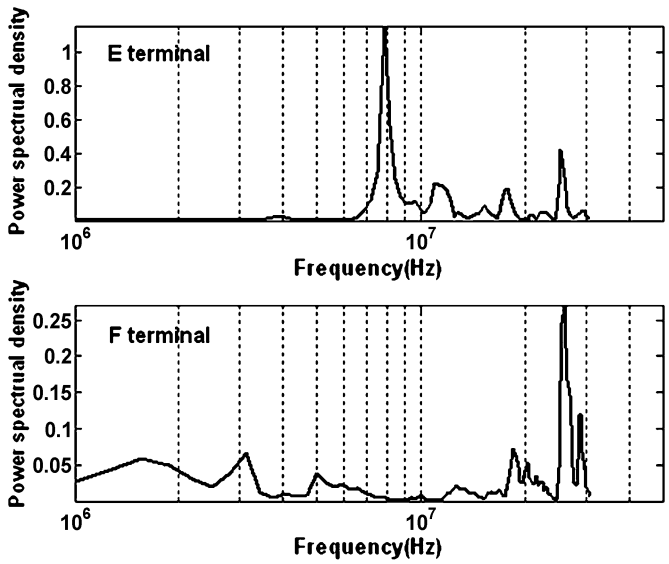

Fig. 5. Frequency response of the simultaneously recorded single PD pulse (17th in Fig. 3) at the E terminal (top) and F terminal of the network (bottom).

and F were analyzed. Randomly occuring detailed single PD pulses were recorded over the duration of 1.6 ms using 100-k sampling points. The typical simultaneously recorded signals at E and F terminals with 1-MΩ termination are shown in Fig. 2. The recorded signal was oscillatory and was decaying with time. Since the occurrence of PD was a random phenomenon, 20 samples of data were analyzed to understand the statistical nature of its individual PD characteristics. In all of the recorded traces, the simultaneous occurrence of PD with some delay was observed at the measuring terminals E and F. The coupled signals at other phases due to this high-frequency PD were not significant. The E terminal time-domain peak response was more than the F terminal response. The sorted positive peak magnitude of individual PDs at the E terminal and the corresponding F terminal and negative peak magnitude at E and F terminals are plotted in Fig. 3. The absolute magnitude of the peak varied from 0.25 to 2.2 V at the E terminal and the corresponding magnitude of the peak at the F terminal varied from 0.25 to 0.9 V.

Using the peak occurrence time as the time delay indicator in 17 cases, the F terminal peak was found to occur with a delay in comparison with the E terminal peak as shown in Fig. 4. The sorted pulse sequence is kept the same from Figs. 3–6. This time delay varied from 10 to 380 ns. The duration of the single PD pulse varied from 1.6 to 3.2 μs. The frequency content of each PD was analyzed. For the time-domain data in Fig. 2, the determined frequency contents for the single PD signal at E and F terminals are shown in Fig. 5. Resonant frequencies of 7.9 and 25 MHz at the E terminal, and 25 MHz at the F terminal occurred. The power spectral magnitude at the F terminal was comparatively less. Since a high-voltage terminal was available, the PD signal was injected at I with and without grounding N. The measured responses at E and F did not vary much with and without grounding N. The peak of the measured response at F increased significantly as shown in Fig. 8. The measured response at E had oscillations for a significant period and the injected peak attenuated significantly. This may be due to the high-frequency impedances of the source and coupling capacitors. The increase

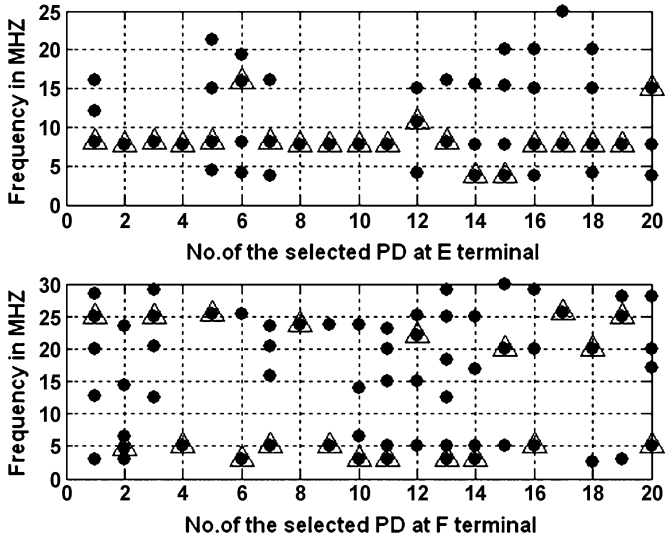

Fig. 6. Observed resonant frequencies at the E and F terminals.

in peak magnitude at F may be due to the significant change in surge impedances of the busbar and the transformer.

A statistical evaluation of the resonant frequencies distribution was made for the 20 sorted pulses. The plot in Fig. 6 shows the distribution of resonant frequencies at the E and F terminals. More high-frequency resonant peaks up to 30 MHz were observed at the F terminal. The characteristic resonance frequencies observed at the E terminal are 3.9, 8, and 15 MHz. At the F terminal, resonant frequencies were observed at 3.5, 5, 20, and 25 MHz. Most likely, one can conclude from the distribution that only one or two types of PD faults occurred. It was also found that for the commutation signal with a duration of 500 μs, the peak-to-peak attenuation between generator (A, C, E) to transformer (B, D, F) was less and there was a significant cross-couping between phases [21].

B. Offline Measurements

When the generator was not energized during the maintenance cycle, the offline measurement was carried out. Using a portable PD pulse source, the PD signal was injected at the neutral (N) of the generator with respect to ground. The simultaneously recorded signals at E and F are shown in Fig. 7. The measured responses attenuated by 50 times and were distorted with oscillation for a longer period. Most of the injected signal dissipated in the generator windings. The measured time-domain peak magnitudes at the E and F terminals were almost the same. The magnitude rose in the order of 0.5–1 μs and then decayed in 3 μs. There was a time delay between the peaks of the injected PD and the observed peak responses. It was 0.45 μs at the E terminal and 0.95 μs at the F terminal.

The magnitude component of the frequencies for the injected PD varies due to an exponential signal. Hence, the transfer-function (TF) analysis using (1) identifies the dominant frequency components of the propagated PD at the measuring nodes. The measured frequency responses for PD injected at N and I are shown in Fig. 9

$$\mathrm{TF} = \frac{\mathrm{PSD}(V_{\mathrm{out}})}{\mathrm{PSD}(V_{\mathrm{in}})}. \tag{1}$$

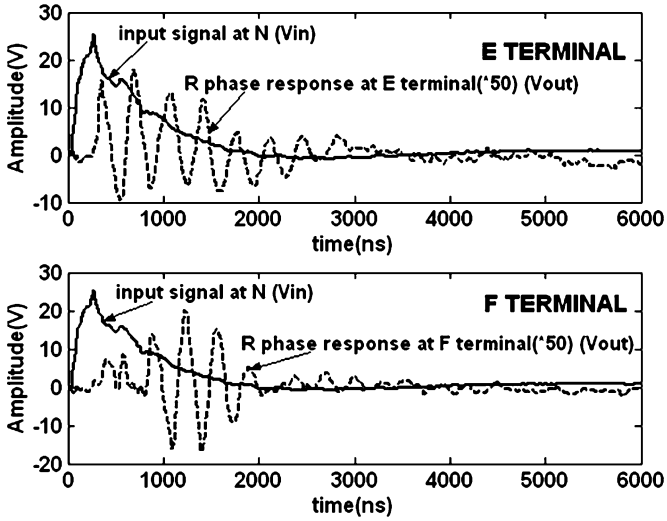

Fig. 7. Measured time-domain responses at E and F for the injected PD at N.

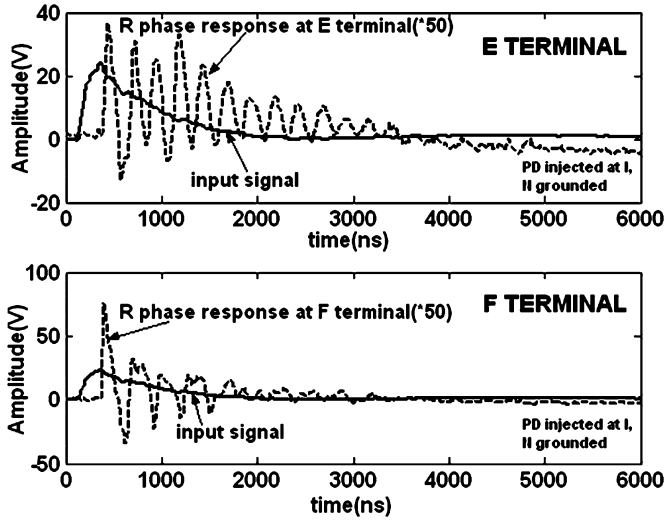

Fig. 8. Measured time-domain responses at E and F for the injected PD at I.

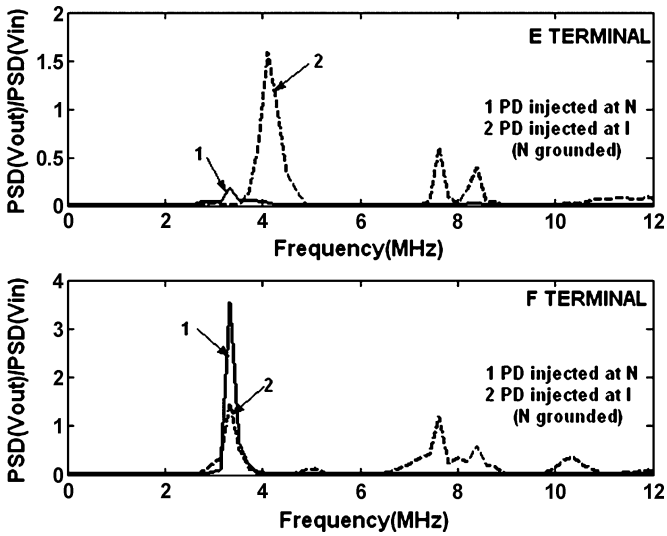

Fig. 9. Calculated transfer-function responses at E and F for the injected PD at N and I.

For the propagation from N to E, the calculated transfer function is found to have resonant frequencies of 3.3 and 8.4 MHz. While for PD propagation from I to E, the resonances change

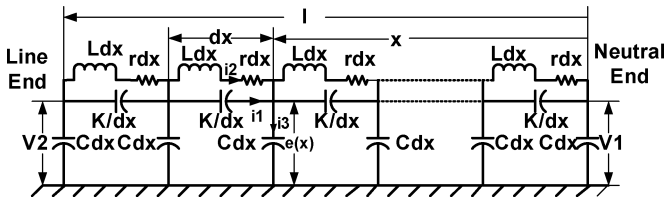

Fig. 10. Transmission-line model of a generator winding.

to 4.1, 7.7, and 8.2 MHz. When PD travels from N to the far away node F, the measured resonant frequencies are 3.3 and 10.2 MHz. For PD travel from I to F, the calculated resonant frequencies are 3.3, 7.7, 8.2, and 10.3 MHz. The high-frequency peaks were not dominant due to the limited high-frequency energy of the perturbing PD source. The above observation suggests that the 3.3-MHz signal is amplified more when it travels from N to F due to resonance in the busbar. For PD traveling from I to E, the resonance peak moves to 4.1 MHz and other minor high-frequency peaks are observed.

The above observations suggest the generation of characteristic resonance peaks. The injected exponential time-domain PD signal gets attenuated by 50 times at the measuring nodes and modulated by the characteristic decaying resonance frequencies. The transfer function analysis identifies these resonance frequencies.

Further research on the propagation model was undertaken to identify the factors causing the attenuation and distortion of PD at two simultaneously measured terminals. The model developed with offline measurement at two nodes was used to predict the possible length of online PD occurrence from the generator windings.

IV. Model Studies

The generator has parallel-connected coils with fewer but longer turns. An analysis was made using a transmission-line model to take into account the series inductance and resistance of the coil, the capacitive coupling between turns, and to ground as shown in Fig. 10.

A. Transmission-Line Model

The distributed series resistance (rdx) and inductance (Ldx) represent the series impedance per section of winding. The parallel capacitance (K/dx) across it along the winding represents the intersection capacitance of turns. The winding insulation capacitance to the grounded slot can be represented by Cdx. The leakage insulation resistance of the winding to ground is very high and is not used in the calculation. V2 is the voltage at the measuring line end terminal and V1 is the voltage at the neutral end where PD is injected. At any length x of the winding length l, the propagating voltage and current can be determined as follows.

At any distance x, the current equations are as follows:

$$i_1 = K\frac{\partial^2 e}{\partial x \partial t} \tag{2}$$

$$i_3 = C\frac{\partial e}{\partial t} = \frac{\partial}{\partial x}(i_1 + i_2). \tag{3}$$

$$\text{Voltage gradient per section} = \frac{\partial e}{\partial x} = L\frac{\partial i_2}{\partial t} + r i_2. \tag{4}$$

Differentiating (4) with respect to x

$$\frac{\partial^2 e}{\partial x^2} = L\frac{\partial^2 i_2}{\partial x \partial t} + r\frac{\partial i_2}{\partial x}. \tag{5}$$

Differentiating (3) with respect to t

$$C\frac{\partial^2 e}{\partial t^2} = \frac{\partial^2 i_1}{\partial x \partial t} + \frac{\partial^2 i_2}{\partial x \partial t}. \tag{6}$$

Rearranging (6)

$$\frac{\partial^2 i_2}{\partial x \partial t} = C\frac{\partial^2 e}{\partial t^2} - \frac{\partial^2 i_1}{\partial x \partial t}. \tag{7}$$

Rearranging (3)

$$\frac{\partial i_2}{\partial x} = C\frac{\partial e}{\partial t} - \frac{\partial i_1}{\partial x}. \tag{8}$$

Substituting (7) and (8) in (5), and using (2)

$$rK\frac{\partial^3 e}{\partial x^2 \partial t} + LK\frac{\partial^4 e}{\partial x^2 \partial t^2} - LC\frac{\partial^2 e}{\partial t^2} - rC\frac{\partial e}{\partial t} + \frac{\partial^2 e}{\partial x^2} = 0. \tag{9}$$

To solve (9), substitute $\partial/\partial t = p$. Equation (9) reduces to (10) as follows:

$$rKp\frac{\partial^2 e}{\partial x^2} + LKp^2\frac{\partial^2 e}{\partial x^2} - LCp^2 - rCp + \frac{\partial^2 e}{\partial x^2} = 0 \tag{10}$$

$$(rKp + LKp^2 + 1)\frac{\partial^2 e}{\partial x^2} = rCp + LCp^2. \tag{11}$$

The solution to (11) is given by (12)

$$\text{Voltage at } x = e(x) = Ae^{\gamma x} + Be^{-\gamma x}. \tag{12}$$

From (3) and (12), the equation for i(x) can be written as

$$i(x) = i_1 + i_2 = \int C\frac{\partial e}{\partial t}dx = \frac{Cp}{\gamma(p)}[Ae^{\gamma x} - Be^{-\gamma x}]. \tag{13}$$

Rewriting (13) in terms of surge impedance (Z)

$$i(x) = \frac{1}{Z}[Ae^{\gamma x} - Be^{-\gamma x}] \tag{14}$$

where

$$\gamma(p) = \sqrt{\frac{LCp^2 + rCp}{LKp^2 + rKp + 1}}$$

$$Z(p) = \frac{\gamma(p)}{Cp}.$$

Substituting $p = j2\pi f = j\omega$ and the quality factor of winding $Q = \omega L/r$, the above terms become a function of frequency

$$\gamma(f) = \frac{j\sqrt{\frac{C}{K}}\sqrt{1 + \frac{1}{jQ}}}{\sqrt{\frac{1}{LK\omega^2} - \frac{1}{jQ} - 1}}$$

$$Z(f) = \frac{\frac{1}{\omega\sqrt{CK}}\sqrt{1 + \frac{1}{jQ}}}{\sqrt{\frac{1}{LK\omega^2} - \frac{1}{jQ} - 1}}. \tag{15}$$

A and B are the constants determined by the terminal conditions. For a winding with open-circuited terminals, the transfer

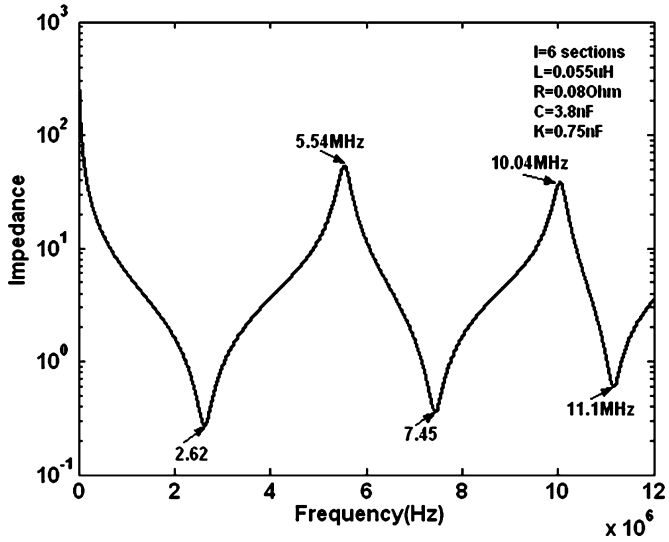

Fig. 11. Variation of Z with frequency.

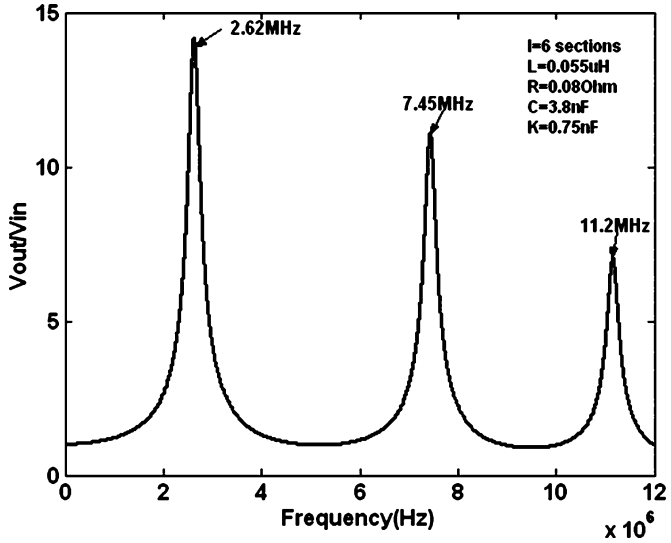

Fig. 12. Variation of $H(f)$ with frequency.

function H (ω) from one end to the other can be determined as follows:

$$H(f) = \frac{V2(f)}{V1(f)}. \tag{16}$$

The terminal conditions are

$$i = 0 \text{ at } x = 0. \tag{17}$$

Substituting (17) in (14) results in $A = B$ and (16) reduces to (18)

$$H(f) = \frac{1}{\cosh(\gamma(p)l)}. \tag{18}$$

This shows that the derived surge impedance and the transfer function will be a function of the frequency. The output response V2 for any perturbation signal V1 can be predicted once the distributed parameters of the generator winding are known. A simple analysis is made by taking six finite sections with $R = 80\ \text{m}\Omega/\text{section}$, $L = 0.055\ \mu\text{H/section}$, $C = 3.8\text{nF/section}$, and $\text{K} = 0.75\ \text{nF/section}$. The surge impedance determined by (15) and transfer function by (18) are shown in Figs. 11 and 12, respectively.

The impedance varies and reaches a minimum value at series resonances of 2.62, 7.45, and 11.1 MHz. The impedance is maximum like a parallel resonance at 5.54 and 10.04 MHz. At the frequency with minimum impedance value, maximum amplification is observed as shown in Fig. 12. The analysis indicates that a finite number of sections may lead to discrete resonance frequencies. This model is extended to the connected network of the measurement setup.

B. Network Model

Since the measurement layout consists of a serially connected generator winding, a busbar and stepup transformer, a network model was developed. The number of transmission-line sections for generator winding and busbar, and the values of distributed parameters of the models on generator, busbar, and stepup transformers were optimized to fit with the experimental measurements. The generator is represented by the transmission-line

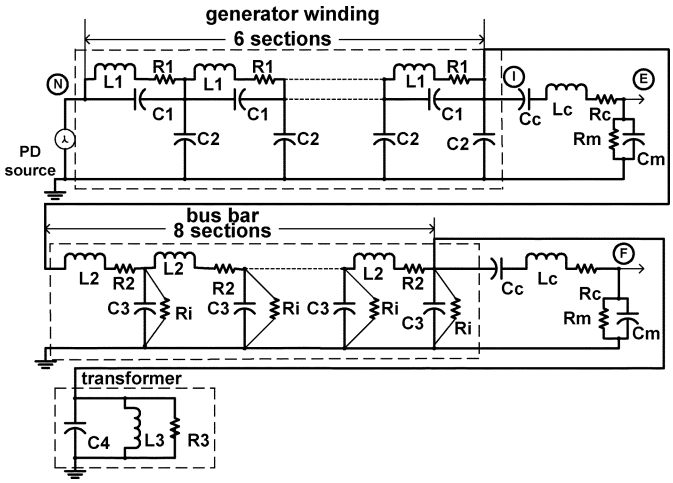

Fig. 13. Network model of generator, busbar, and transformer.

network shown in Fig. 13. For the busbar, interturn capacitance is not included. The terminating step-up transformer is modeled like a parallel-connected RLC lumped circuit since the PD is not monitored in the transformer windings. In addition, the coupling capacitor model with the measuring resistor at the two ends of the busbar is incorporated. PSpice [22] was used for the simulation study to match the various measurements.

1) PD Injected at N: Since the dominant number of peaks in the online observations was around 5, the number of sections was kept around that number. The parameters were tuned in such a way as to match the measured time-domain responses at E and F. The match was terminated on reaching the maximum correlation factors of 0.94 and 0.95 between the measured and simulated results at E and F, respectively. For the injected PD at N, the time-domain results are shown in Fig. 14.

The measured time-domain response at the E terminal had a peak voltage of around 0.35 V and a pulse duration of 3 μs, and the simulated response had a peak voltage of 0.45 V and a pulse duration of 3 μs. While at the F terminal, the measured peak was around 0.4 V with a pulse duration of 3.5 μs. The simulated peak was around 0.42 V with a pulse duration of 3.5 μs.

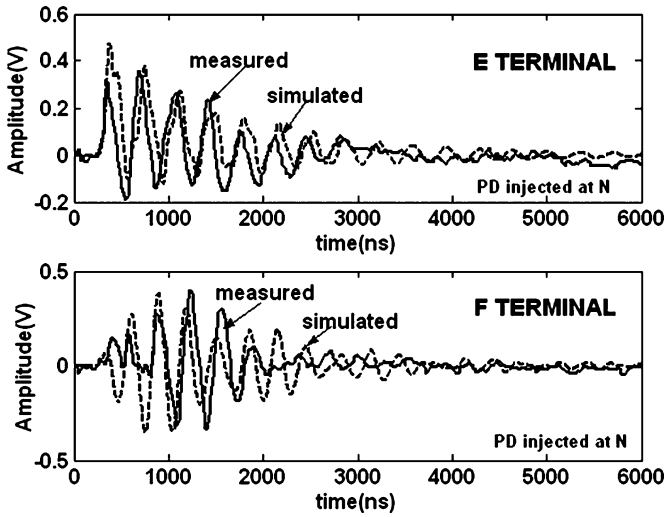

Fig. 14. Measured and simulated time-domain responses at E and F for the injected PD at N.

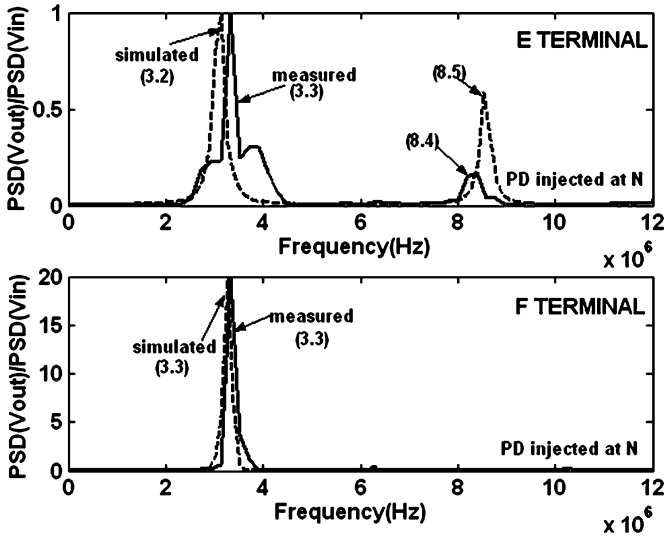

Fig. 15. Measured and simulated frequency-domain responses at E and F for the injected PD at N.

Further analysis on the quality of fitting is tested on the frequency-domain responses shown in Fig. 15. The measured and simulated frequencies matched closely at E and F.

2) PD Injected at I: The same network model was used to predict the responses at E and F for the injected PD at I terminal. More attention was paid to matching the resonance frequencies with the developed model. The frequency-response plot shown in Fig. 16 shows the matching only at the lowest resonance frequency. Near the injection node I, E had a high-frequency content of 4.1 MHz while at F, the matched dominant low frequency moved to 3.3 MHz.

The effect of grounding N did not alter the measurement much. After validating the model for predicting the responses at E and F for the injected PD at N and I, analysis was extended to predict the location of PD for online data.

V. Prediction of PD Location

The main objective of developing a network model was to identify the possible origin location of the PD and the type of PD.

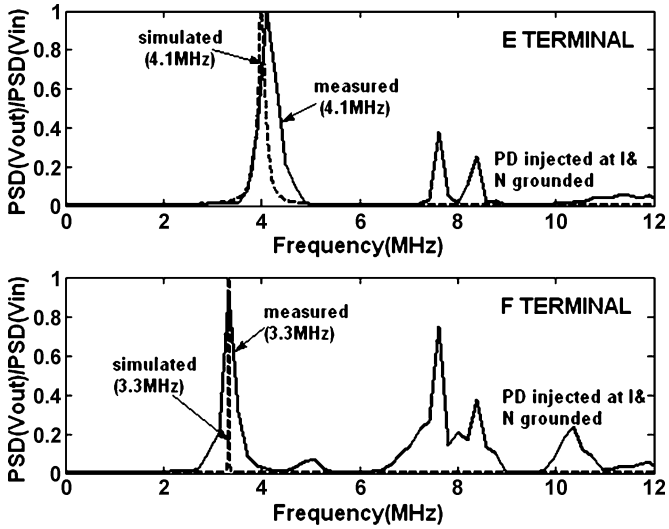

Fig. 16. Measured and simulated frequency-domain responses at E and F for the injected PD at I.

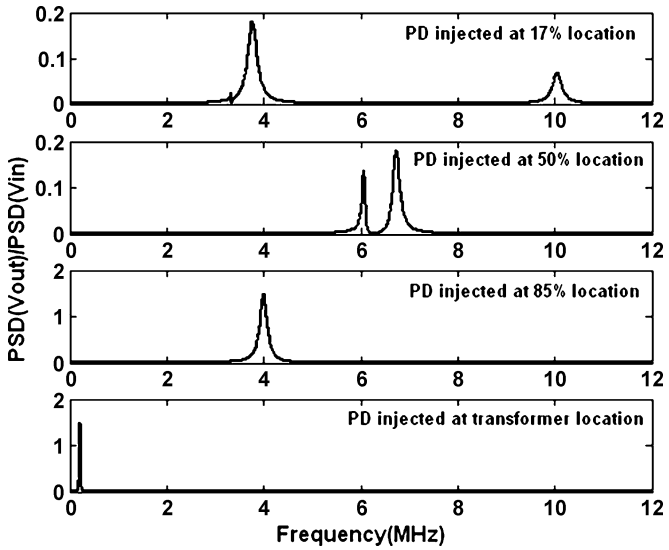

Fig. 17. Predicted frequency responses at E.

1) PD Injected at Various Locations: Since the generator winding is modeled with six sections, the responses at E and F for the injected PD at N, 17%, 33%, 50%, 67%, 83%, and 100% of generator windings and transformers can be predicted using the developed model. For more clarity, typical results at E and F are presented in Figs. 17 and 18, respectively. In Fig. 17, the resonant frequencies and their magnitudes varied with location. For the origin of the PD at 17% and 50% of the generator winding, two resonant frequencies with low amplitude are observed. As the origin moves closer to the measuring terminal, the magnitude rises with one dominant low frequency peak. For the injected PD from the transformer in the form of noise, only a dominant very low frequency is observed.

In Fig. 18, a significant increase in the signal is obtained due to a resonance in the busbar propagation path. The resulting resonance frequencies varied with the location of the PD. As the monitoring node moves away, the resonance frequencies move to a low-frequency range.

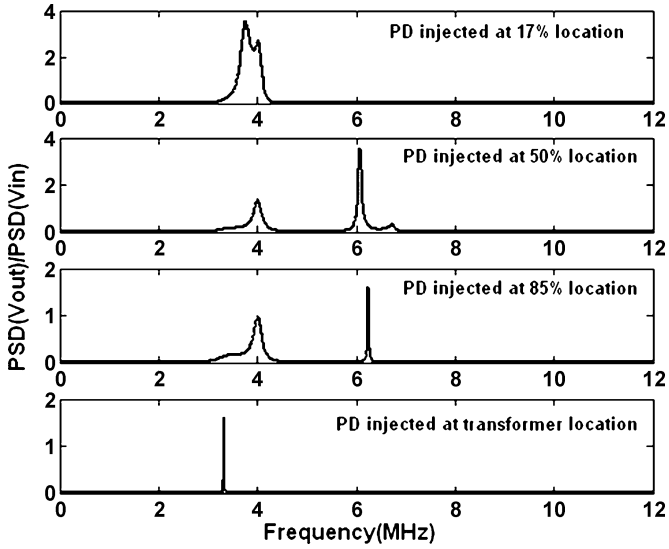

Fig. 18. Predicted frequency responses at F.

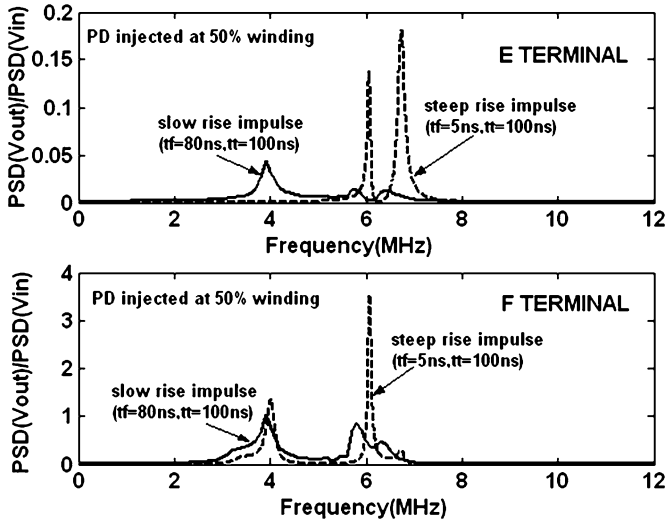

Fig. 19. Effect of the PD waveshape.

2) PD Waveshape: In this analysis, the injected PD location is fixed at 50% of the generator winding. PDs with rise times of 5 and 80 ns and with a fall time of 100 ns are injected. It was found that the dominant high-frequency responses at E and F can be obtained with fast rising impulses in Fig. 19.

The reason for this is that the high-frequency components of the fast rising impulse are more than the slow rising impulse. The propagation mode is more complicated.

A simple correlated study on the observed online measurements shown in Fig. 6 suggests that most PDs may have originated around 85% into the generator winding.

VI. Conclusion

In this work, it was found that portable PD pulse sources using a mercury switch can be used to generate and study the propagation of PD pulses in an offline mode on a 250-MVA-rated generator in a connected power network. A computerized online high-frequency multichannel simultaneous measurement system can be used for PD propagation studies at the generator of a power plant. The online and offline testing results were analyzed in the time and the frequency domains. It was found from online measurements that single PD propagation in the power network was very complicated and may result in characteristic resonance frequencies with attenuation depending on the distance from origin to the measuring location. The model that fits in matching the testing results was analyzed. The generator winding, the busbar, and the connected high-voltage (HV) transformer all contribute to the complicated propagation phenomena.

It is concluded that the proposed off and online PD measurements can be used to identify the PD propagation model and associated parameters of that particular power network. Very satisfactory fitting of experimental observations with the model suggests that this approach can be used effectively to predict the roles of PD originating from different locations of the power network and to estimate the distortion of different original PD waveshapes. The developed model could be used to locate the position of the PD source if one gets simultaneous single PD recordings from two locations of the same phase.

References

[1] *IEEE Trial-Use Guide to the Measurement of Partial Discharges in Rotating Machinery*, IEEE Std. 1434-2000, 2000.

[2] G. Stone, "Importance of bandwidth in PD measurement in operating motors and generators," *IEEE Trans. Dielectr. Elect. Insul.*, vol. 7, no. 1, pp. 6–11, Feb. 2000.

[3] G. C. Stone, "Partial discharge part XXV: Calibration of PD measurements for motor and generator windings–Why it can't be done," *IEEE Electr. Insul. Mag.*, vol. 14, no. 1, p. 9, Jan./Feb. 1998.

[4] G. C. Stone and P. Kantardziski, "Partial discharge testing of motor and generator windings: An absolute or a comparison test," in *Proc. IEEE Int. Symp. Electr. Insulating Materials*, 1998, pp. 63–66.

[5] X. Dong, D. Zhu, C. Wang, and K. Tan, "Simulation of transformer PD pulse propagation and monitoring for a 500 kV substation," *IEEE Trans. Dielect. Electr. Insul.*, vol. 6, no. 6, pp. 803–813, Dec. 1999.

[6] Z. D. Wang, P. A. Crossley, K. J. Cornick, and D. H. Zhu, "An algorithm for partial discharge location in distribution power transformers," in *Proc. IEEE Power Eng. Soc. Winter Meeting*, 2000, pp. 2217–2222.

[7] Z. D. Wang and D. H. Zhu, "Simulation on propagation of partial discharge pulses in transformer windings," in *Proc. IEEE Int. Symp. Electrical Insulating Material*, Toyohashi, Japan, Sep. 1998, pp. 643–646.

[8] Z. D. Wang, P. A. Crossley, and K. J. Cornick, "A simulation model for propagation of partial discharge pulses in transformers," in *Proc. IEEE Power System Technology*, 1998, pp. 151–154.

[9] S. N. Hettiwatte, P. A. Crossley, Z. D. Wang, A. Darwin, and G. Edwards, "Simulation of a transformer winding for partial discharge propagation studies," in *Proc. IEEE Power Eng. Soc. Winter Meeting*, 2002, pp. 1394–1399.

[10] H. J. van Breen, E. Gulski, J. J. Smit, H. F. A. Verhaat, W. de Leeuw, and M. Krieg-Wezelenberg, "Standardization of on-line VHF PD measurements on turbo generators," in *IEEE Trans. Dielect. Elect. Insul.*, vol. 9, Feb. 2002, pp. 140–149.

[11] J. W. Wood, H. G. Sedding, W. K. Hogg, I. J. Kemp, and H. Zhu, "Partial discharges in HV machines; initial consideration for a PD specification," in *Proc. IEEE 6th Int. Conf. Dielectric Materials, Measurements Applications*, 1992, pp. 154–157.

[12] Q. Su, "Analysis of partial discharge pulse propagation along generator stator windings," in *Proc. IEEE Power Eng. Soc. Winter Meeting*, 2000, pp. 269–272.

[13] A. J. M. Pemen, P. C. T. van der Laan, and W. de Leeuw, "Analysis and localization of spurious partial discharge activity in generator units," in *Proc. IEEE 7th Int. Conf. Solid Dielectrics*, 2001, pp. 489–492.

[14] J. Fuhr, M. Haessig, P. Boss, D. Tschudi, and R. A. King, "Detection and location of internal defects in the insulation of power transformers," *IEEE Trans. Electr. Insul.*, vol. 28, no. 6, pp. 1057–1067, Dec. 1993.

[15] E. P. Dick, R. W. Cheung, and J. W. Poter, "Generator models for over voltage simulation," *IEEE Trans. Power Del.*, vol. 6, no. 2, pp. 728–735, Apr. 1991.

[16] A. Narang, B. K. Gupta, E. P. Dick, and D. Sharma, "Measurement and analysis of surge distribution in motor stator windings," *IEEE Trans. Energy Convers.*, vol. 4, no. 1, pp. 126–134, Mar. 1989.
[17] B. Heller and A. Veverka, *Surge Phenomena in Electrical Machines*. London, U.K.: London Iliffe Books Ltd., 1968, pp. 364–387.
[18] A. Greenwood, *Electrical Transients in Power Systems*. New York: Wiley, 1971, pp. 251–280.
[19] P. Chowdhuri, *Electromagnetic Transients in Power Systems*. New York: Wiley, 1996, pp. 241–281.
[20] S. Birlasekaran, "Identification of the type of partial discharges in an operating 16 kV/250 MVA generator," in *Proc. IEEE Conf. Electrical Insulation Dielectric Phenomena*, Albuquerque, NM, 2003, pp. 559–562.
[21] S. Z. Qin, S. Birlasekaran, and C. L. Shih, "Study of partial discharge and attenuation from an operating 250 MVA generator," *EEE Res. Bull.*, pp. 86–87, 2003.
[22] Cadence, PSpice Ver. 9.1.

Qin Shaozhen received the B.Sc. and M.Eng. degrees in electrical engineering from Xi'an Jiaotong University, Xi'an, China, in 1993 and 1996, respectively. He is currently pursuing the Ph.D degree in the field of power apparatus condition monitoring, Nanyang Technological University, Singapore.

From 1996 to 1998, he was a Research Engineer with North West Electrical Power Research Institution (NWEPRI), where he was involved in electrical instrument development and high-voltage equipment preventive testing. From 1998 to 2001, he was a Senior Engineer with the Shaanxi Electrical Power Corporation, Xi'an, having worked on power equipment insulation fault analysis. Since 2004, he has been the Executive Engineer with Singapore Power Power Grid (SPPG), taking on electrical equipment condition monitoring duties. His interests are in the areas of electrical measurement and power equipment fault diagnosis.

Mr. Shaozhen was a member of the Chinese Standards Committee TC65 on HV Switchgear from 1998 to 2001.

S. Birlasekaran (SM'98) received the M.E. degree (Hons.) from the Indian Institute of Science (IISC), Bangalore, India, in 1970, and the Ph.D. degree in high voltage engineering from the University of Queensland, Queensland, Qld., Australia, in 1980.

Currently, he is an Associate Professor with Nanyang Technological University. From 1970 to 1998, he was with the R&D HV Laboratories, University of New Castle, New Castle, NSW, Australia; University of Bombay, Bombay, India; IISC; Central Electrochemical Research Institute, Karaikudi, India; National Measurements Laboratory, Council of Scientific and Industrial Research Organisation, Lindfield, Sydney, Australia; National Measurements Laboratory (NML), Council of Scientific and Industrial Research Organization, Lindfield, Sydney, Australia; Sydney, and Electrodata Sydney, Sydney, Australia, at various levels. He was actively engaged in developing various condition monitoring techniques associated with power utilities in the Australia—Electricity Commission of NSW, Southern Electric Authority of Queensland (SEAQ), Brisbane, Australia; Pacific Power, New Castle, Australia; and North Power, Singleton, NSW, Australia, and with various utilities in Singapore, Malaysia, and Indonesia.

Dr. Birlasekaran is a Professional Engineer in Singapore and a member of TCs on Singapore Standards on power apparatus.